

Influence of charge-carrier density on the magnetic and magnetotransport properties of $\text{Tl}_{2-x}\text{Cd}_x\text{Mn}_2\text{O}_7$ pyrochlores ($x \leq 0.2$)

P. Velasco,¹ J. A. Alonso,¹ M. T. Casais,¹ M. J. Martínez-Lope,¹ J. L. Martínez,¹ and M. T. Fernández-Díaz²

¹*Instituto de Ciencia de Materiales de Madrid (CSIC), Cantoblanco, 28049 Madrid, Spain*

²*Institut Laue-Langevin, Boîte Postal 156, F-38042 Grenoble Cedex 9, France*

(Received 18 December 2001; revised manuscript received 25 March 2002; published 5 November 2002)

Three members of the pyrochlore series $\text{Tl}_{2-x}\text{Cd}_x\text{Mn}_2\text{O}_7$ ($0 \leq x \leq 0.2$), prepared under high pressure, have been characterized by neutron powder diffraction, susceptibility, specific heat, magnetotransport, and Hall measurements. The materials are ferromagnetic, and the Curie temperatures (T_C) slowly decrease upon Cd substitution, as a consequence of the progressive reduction of Mn-O-Mn superexchange interactions. Both electrical resistance and magnetoresistance (MR) are dramatically enhanced with respect to stoichiometric $\text{Tl}_2\text{Mn}_2\text{O}_7$, due to the significant reduction in the number of carriers (electrons) induced by hole doping, measured from Hall data. In particular, MR(9 T) reaches an unprecedented value of 10⁶% at 120 K for the $x=0.2$ compound. We have analyzed the conduction mechanism in the region above T_C in terms of polaron hopping. The presence of polarons is also evidenced from the deviations to the Curie-Weiss fits above T_C . We suggest that the large increase of MR and the observed weakening of the magnetic interactions are both related to the decrease in the number of carriers.

DOI: 10.1103/PhysRevB.66.174408

PACS number(s): 75.30.Vn, 75.50.-y

I. INTRODUCTION

Colossal Magnetoresistance (CMR) has attracted a lot of attention since its discovery in hole-doped perovskite manganites ($R_{1-x}A_x\text{MnO}_3$, with R =rare earths, A =alkali earths).¹ This effect can be described as the change of the electrical resistance upon the application of an external magnetic field. The possible applications based on these compounds, mainly as magnetic sensors, have triggered an intense effort oriented to fully understand this phenomenon. The main ingredient for the CMR in these materials is the presence of Mn cations in a mixed $\text{Mn}^{3+}/\text{Mn}^{4+}$ valence state. This mixed valence leads to a magnetic double exchange (DE) that, together with a strong electron-lattice coupling, is responsible for the change of resistance between the magnetically ordered and disordered states. Near and above the transition temperature T_C , where the disordered state can be easily driven to an ordered state by the application of a magnetic field, “colossal” values for the magnetoresistance (MR) ratio are found.

CMR has also been reported in other nonperovskite oxides, such as the $\text{Tl}_2\text{Mn}_2\text{O}_7$ pyrochlore.²⁻⁴ Although, by far, it has been much less studied than perovskite manganites, given the difficulties inherent to its high pressure synthesis, some effort has been devoted to understand the mechanisms driving the electronic conduction and ferromagnetism,⁴⁻⁷ as well as to improve the observed MR ratio and the transition temperature.

$\text{Tl}_2\text{Mn}_2\text{O}_7$ is a ferromagnetic (FM) oxide, with a T_C of about 125 K. The room-temperature resistance is in the order of 10 Ω cm, evidencing the low density of carriers involved in the transport phenomena ($n \sim 0.005 e^-/\text{unit cell}^2$). As the pyrochlore structure $A_2B_2O_7$ is able to incorporate a large number of different cations,⁸ some substitutions have been carried out in $\text{Tl}_2\text{Mn}_2\text{O}_7$, both at the Tl and the Mn positions, in order to gain additional information from the

changes experienced in the physical properties upon doping. Thus, In,³ Sc,⁵ Bi,⁹ and Cd (Ref. 10) have been successfully introduced at the Tl positions. And the Mn atoms have been replaced by Ru,¹¹ Sb,¹² Te,¹³ and Ti.¹⁴ The introduction of Sb and Te led to a significant increase in the transition temperature (T_C), although, as a drawback, the MR ratio was reduced. On the other hand, higher MR has been found for the Bi and Cd substitutions. To our knowledge, the highest MR ratio ever reported was found for the $\text{Tl}_{1.8}\text{Cd}_{0.2}\text{Mn}_2\text{O}_7$ pyrochlore. This material was the object of a previous letter,¹⁰ where a MR as high as 10⁶% at 9 T was described at 120 K.

In this work we present a more detailed report of the in-depth study that was carried out in the $\text{Tl}_{2-x}\text{Cd}_x\text{Mn}_2\text{O}_7$ $0 \leq x \leq 0.2$ series, including structural data from x-ray diffraction (XRD) and neutron powder diffraction (NPD); magnetic data, resistance, and magnetoresistance analysis; Hall-effect measurements and specific heat data; as well as a global interpretation in terms of the relationship between the charge-carrier density and the magnetotransport properties. We will also discuss on the necessity of considering a $\text{Mn}^{4+}/\text{Mn}^{5+}$ valence mixing, due to the partial replacement of Tl^{3+} by aliovalent Cd^{2+} cations.

II. EXPERIMENTAL

High-pressure and high-temperature conditions are required to prepare these compounds. Nominal $\text{Tl}_{2-x}\text{Cd}_x\text{Mn}_2\text{O}_7$ ($x=0.0, 0.1, \text{ and } 0.2$) pyrochlores were synthesized from stoichiometric mixtures of Tl_2O_3 , CdO , and MnO_2 powders. The mixtures of oxides were packed into a 8-mm-diameter gold capsule, placed in a cylindrical graphite heater. The reaction was carried out in a piston-cylinder press, at a pressure of 20 kbar at 1300 K for 1 h. The reaction products, in the form of blackish dense polycrystalline pellets, were partially ground for XRD characterization, with $\text{Cu } K_\alpha$ radiation. All of the XRD reflections could be indexed in a cubic unit cell as single-phase pyrochlore, as

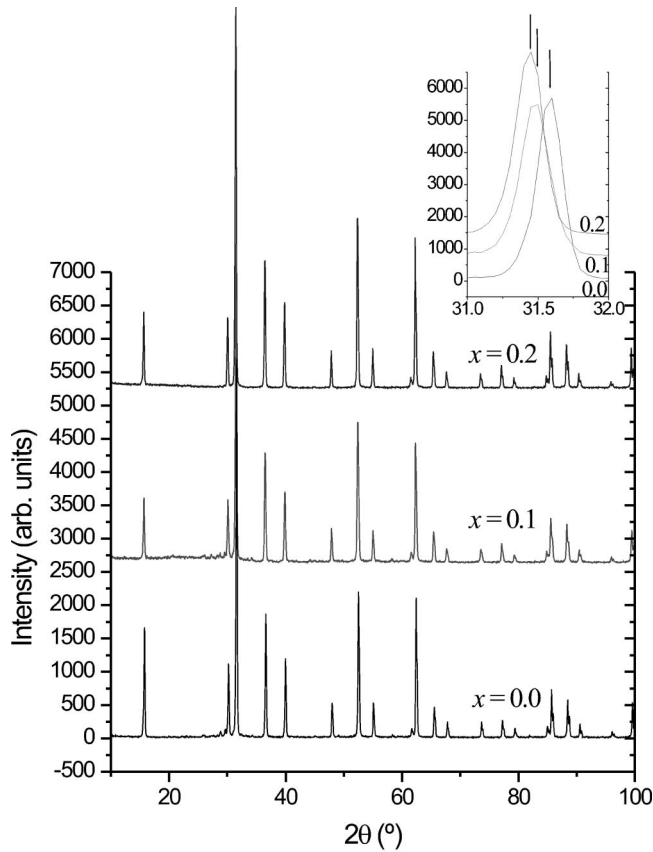


FIG. 1. XRD spectra for the $Tl_{2-x}Cd_xMn_2O_7$ compounds. They correspond to a single-phase pyrochlores. Inset: detailed view of the most intense reflection (222), showing a displacement to lower angles with Cd doping (arrows show the maximum of the peak). This shift corresponds to an increase of the lattice parameter.

shown in Fig. 1. The variation of the unit cell parameter is almost linear, from $a = 9.9004(1)$ Å for $Tl_2Mn_2O_7$, to $a = 9.9075(1)$ Å for $Tl_{1.8}Cd_{0.2}Mn_2O_7$. This variation is consistent with the larger ionic radius for Cd^{2+} (1.10 Å) than for Tl^{3+} (0.98 Å) in eightfold coordination¹⁵ (Cd^{2+} is well known to occupy the *A* positions in many pyrochlores⁸). The inset shows the displacement of the most intense reflection (222) with doping.

A NPD study was performed at room temperature for the Cd-rich end of the series $x=0.2$ (see Fig. 2). The high-resolution spectrum was recorded at the D2B diffractometer of the ILL (Grenoble), with a wavelength $\lambda = 1.594$ Å. The sample, weighing 0.8 g, was packed in a double-walled vanadium holder, to minimize the Cd absorption. The NPD pattern was Rietveld refined using the FULLPROF program.¹⁶ The structural model was that of the conventional cubic pyrochlore, defined in the space group $Fd\bar{3}m$, $Z=8$. Tl and Cd atoms were considered to be randomly distributed at the *A* positions. The results are summarized in Table I. The final crystallographic composition is $[Tl_{1.73(2)}Cd_{0.27(2)}]_c sites [Mn_2]_d sites O_{7.01(1)}$. There is no measurable oxygen deficiency at *O'* positions. The Mn-O distance observed for $Tl_{1.8}Cd_{0.2}Mn_2O_7$, of 1.8983(8) Å, is significantly shorter than that observed for the nonsubstituted pyrochlore, of 1.9013(4) Å,¹⁷ in spite of the expansion observed in the unit-cell volume. This is due to the significant change of the x parameter for *O* oxygen positions [$x=0.4245(8)$ in the undoped compound¹⁷], and it is consistent with the strengthening of the Mn-O bonds due to the removal of electrons from bands of antibonding character.

Magnetic dc susceptibility and magnetization were measured in a commercial superconductor quantum interfero-

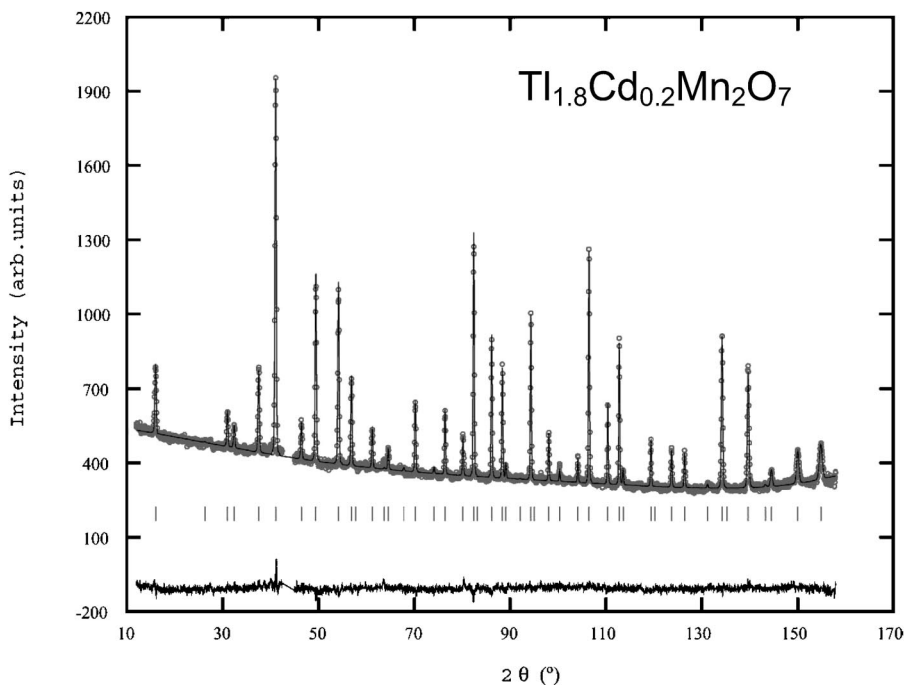


FIG. 2. Observed (open circles), calculated (full line), and difference (bottom) NPD Rietveld profiles for $Tl_{1.8}Cd_{0.2}Mn_2O_7$. The series of tick marks correspond to the allowed Bragg reflections.

TABLE I. Atomic parameters after the Rietveld analysis of the $x=0.2$ compound, from NPD data at RT, refined in the $Fd\bar{3}m$ space group $a=9.9075(1)$ Å. The main interatomic distances (Å) and angles ($^\circ$) are also included. Agreement factors: $R_p=2.10\%$, $R_{wp}=2.68\%$, $R_f=7.01\%$, $\chi_2=2.35$.

Atom	site	x	y	z	f_{occ}^a	$B(\text{Å}^2)$
Tl	16c	0	0	0	0.87(1)	0.65(4)
Cd	16c	0	0	0	0.13(1)	0.65(4)
Mn	16d	0.5	0.5	0.5	1.0	0.68(8)
O	48f	0.4258(1)	0.125	0.125	1.0	0.79(2)
O'	8a	0.125	0.125	0.125	1.01(1)	0.51(8)
Mn-O		1.8983(8)		Mn-O-Mn	134.44	
Tl-O		2.4681(8)				
Tl-O'		2.1436(1)				

^aThe refinement of the occupancy factors leads to a crystallographic composition $[\text{Tl}_{1.73(2)}\text{Cd}_{0.27(2)}]_c \text{ sites} [\text{Mn}_2]_d \text{ sites} \text{O}_{7.01(1)}$.

meter device (SQUID) in magnetic fields up to 5 T, and temperatures from 2 to 400 K. Resistance and magnetoresistance data were measured in a conventional four-points configuration, in a physical properties measurement system (PPMS) from Quantum Design, in magnetic fields up to 9 T and temperatures from 5 to 400 K. Hall-effect data were collected in a five-points configuration. This configuration allows us to eliminate from the data any longitudinal contribution that could have been introduced by the somewhat irregular geometry of the pellets. Also the contribution from the MR was compensated before performing the Hall analysis. The specific heat measurements were also carried out in a PPMS, by the quasiadiabatic heat pulses relaxation method. The estimated resolution is better than 1%.

III. RESULTS

Figure 3 condenses the magnetic measurements carried out in the samples. In the left axis we present the dc suscep-

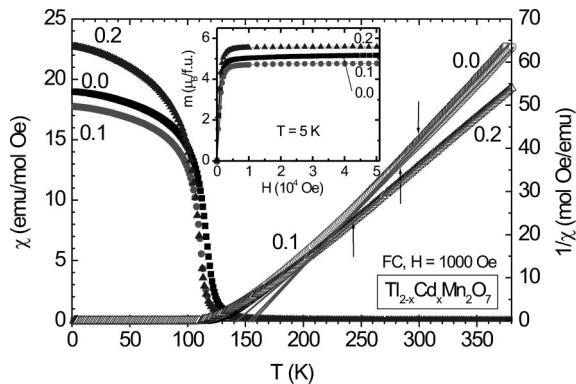


FIG. 3. Magnetic data for the $\text{Tl}_{2-x}\text{Cd}_x\text{Mn}_2\text{O}_7$ oxides. Left axis: Susceptibility, measured at 1000 Oe after a field-cooled process. Right axis: Inverse of the susceptibility, together with the linear fit to a Curie-Weiss behavior. Arrows mark the points where the data separate from the ideal law. Inset: positive branches of the magnetization at 5 K.

TABLE II. Magnetic parameters for the $\text{Tl}_{2-x}\text{Cd}_x\text{Mn}_2\text{O}_7$ compounds.

Sample	T_C (K)	M_S ($\mu_B/\text{f.u.}$)	θ_{CW} (K)	μ_{eff} ($\mu_B/\text{f.u.}$)
0.0	118	5.185	154	5.20
0.1	112	4.733	151	5.28
0.2	110	5.558	141	5.40

tibility, measured in a 1000 Oe field, after a field-cooled process. The samples are $\text{Tl}_2\text{Mn}_2\text{O}_7$ (labeled as “0.0”), $\text{Tl}_{1.9}\text{Cd}_{0.1}\text{Mn}_2\text{O}_7$ (“0.1”), and $\text{Tl}_{1.8}\text{Cd}_{0.2}\text{Mn}_2\text{O}_7$ (“0.2”). All the three samples show the spontaneous magnetization characteristic of FM materials, with a transition temperature that decreases with doping (see Table II). This observation suggests a decrease in the strength of the FM interactions. The inverse of the susceptibility (right axis) follows a Curie-Weiss behavior, but only for high temperatures, well above T_C . The Weiss temperature (θ_W) decreases when increasing the Cd doping level, in agreement with the reduction of the magnetic interactions that can be inferred from the T_C values.

When cooling from high temperatures, a deviation from the Curie-Weiss linear dependence is observed. This fact has been attributed to the presence of spin polarons above T_C . A spin polaron is a FM cluster in the paramagnetic region, where an electron is captured. It has been shown that a FM alignment of the localized magnetic moments favors the mobility of the conduction electrons²⁻⁴ in this family of compounds. Therefore, the formation of FM clusters is favored by a decrease in the kinetic energy of the carriers. As the temperature is increased from the FM region, above but close to T_C the formation of spin polarons is easy: although the long-range magnetic interactions are vanished, there still remain short-range interactions. As temperature increases, the thermal energy finally overcomes the kinetic energy gain, destroying the short-range interactions, and reaching the PM regime. This PM regime corresponds in the graph (Fig. 3) to the solid lines that are coincident with the inverse of the susceptibility only above a certain temperature. The temperature of deviation is marked for each sample with an arrow. The left-most one corresponds to $\text{Tl}_{1.8}\text{Cd}_{0.2}\text{Mn}_2\text{O}_7$, while the rightmost one corresponds to the pure $\text{Tl}_2\text{Mn}_2\text{O}_7$ compound, being the middle one the corresponding to the $\text{Tl}_{1.9}\text{Cd}_{0.1}\text{Mn}_2\text{O}_7$. The temperature of formation of polarons is lowered with increasing the Cd doping, which means that the short-range magnetic interactions also are weakened.

The inset of Fig. 3 shows the magnetization curves at 5 K. They are characteristic of a FM behavior, with a low saturation field (a 98% of the saturation value is reached for a 0.5 T field). The remanent field is also very small (of the order of 10 Oe). The value of the saturation magnetization (Table II) increases with the Cd doping.

The thermal variation of the resistivity is plotted in the lower panel of Fig. 4, both with (open symbols) and without (solid symbols) an applied magnetic field (9 T). In the absence of magnetic field, an insulator-type behavior is observed for temperatures well above T_C . By decreasing the temperature below 200 K, a huge drop in the resistivity is

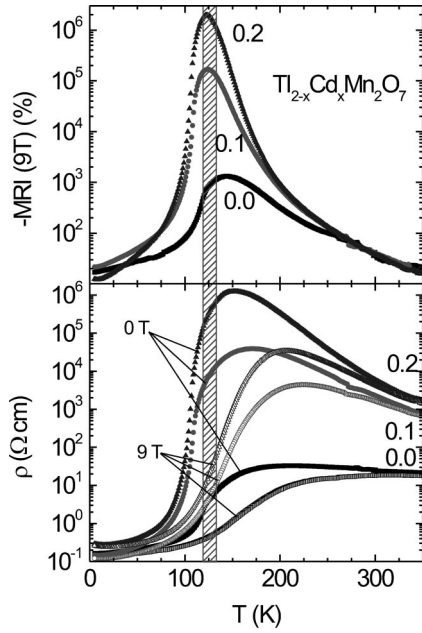


FIG. 4. Lower panel: variation of the resistivity with the temperature for $\text{Ti}_{2-x}\text{Cd}_x\text{Mn}_2\text{O}_7$, both with (open symbols) and without (solid symbols) applied magnetic field of 9 T. Upper panel: dependence of the magnetoresistance with the temperature (see the text for MRI definition). The shadowed area represents the zone where the magnetic transition takes place.

observed, leading to a metallic behavior for low temperatures. This metal-insulator transition is concomitant with the magnetic transition (the magnetic transition temperatures lay in the shadowed temperature interval), and it is related to the kinetic energy gain by the conduction electrons when the neighboring localized moments become ferromagnetically ordered. Roughly speaking, a high-resistance state is found in the PM region, and the low-resistance state is observed in the FM region, with a wide transition between them. The fact that this transition is not a sharp one is explained by the wide PM region in which an appreciable contribution to the susceptibility comes from the presence of spin polarons. There is a large difference between the resistivity magnitudes of the three studied samples; the room-temperature values are included in Table III. This difference cannot be explained by only considering the magnetic interactions from one sample to the others. As it can be seen in Fig. 3, the values in the inverse of the susceptibility (and, hence, in the susceptibility itself) are not very far from one another. At least not to justify a two order of magnitude increase in the room temperature resistivities. This fact is, then, related either to a decrease in the number of carriers, as we found from Hall-effect measurements, described below; or to a decrease in the

mobility. This will be discussed later. The magnitude of the high-temperature to low-temperature drop is also strongly sample dependent, as shown in Table III. The differences in the ratio of resistivity between the high-resistive and the low-resistive regions $\rho_{200\text{K}}/\rho_{50\text{K}}$ increase with the degree of Cd doping. This fact can be accounted for by considering the concomitant changes in the number of carriers, in such a way the samples with a lower number of carriers (and higher Cd doping) are more affected by the magnetic interactions.

We analyzed the conduction mechanism in the region above T_C in terms of polaron hopping. In this case, the resistivity in that region should be thermally activated,¹⁹ in the form

$$\sigma = \sigma_0 \exp\left(-\frac{E_\sigma}{k_B T}\right),$$

where $\sigma_0 = g_d e^2 \nu_0 \delta / a k_B T$. The factor g_d is determined by the hopping geometry, ν_0 and a are the attempt frequency and hopping distance, respectively, and δ is the carrier concentration per Mn site. Consequently, we have fitted the high-temperature resistivity data for the three samples for such an activated behavior. The good agreement of the fits is consistent with the existence of spin polarons for such temperatures. This also demonstrates that polarons are responsible for the conduction in the insulator region. The values found for E_σ are given in Table III. As it can be seen, there is an increase in E_σ upon Cd doping. That means that as the Cd content increases, it becomes more difficult for the polarons to hop from one position to a neighboring one. In fact, the energetic barrier they have to jump over is higher. This energetic barrier reflects the difficulty of polarizing in parallel the localized magnetic moments surrounding the polaron, and, hence, allowing the polaron to move to the next position. In other words, the increase in the E_σ values again evidences a decrease in the strength of the FM interactions when we replace Ti by Cd, as it was shown by the decrease in T_C .

When a magnetic field is applied, the localized Mn^{4+} magnetic moments tend to align parallel to the field, diminishing the scattering of the carriers and, thus, increasing the mobility of the conduction electrons. This fact is manifested in a decrease of the resistivity, as shown in the lower panel of Fig. 4 (open symbols). The effect is more drastic in the vicinity of the magnetic transition. In this region, the application of a magnetic field aligns in parallel the localized moments, the corresponding thermal energy being unable to disorder them. For higher temperatures (close to room temperature) this effect is reduced by the thermal agitation.

TABLE III. Transport and magnetotransport parameters.

Sample	$\rho_{300\text{K}}$ (Ωcm)	$\rho_{200\text{K}}/\rho_{50\text{K}}$	T_{max} (K)	E_σ (meV)	$C_{\text{Littlewood}}$	n_{Hall} ($e^-/\text{u.c.}$)
0.0	25.67	154.7	144	55.4	48.39	5.5×10^{-3}
0.1	2244.5	1.16×10^5	124	214.3	75.20	1.51×10^{-3}
0.2	5951.3	8.78×10^5	122	265.1	91.88	1.97×10^{-4}

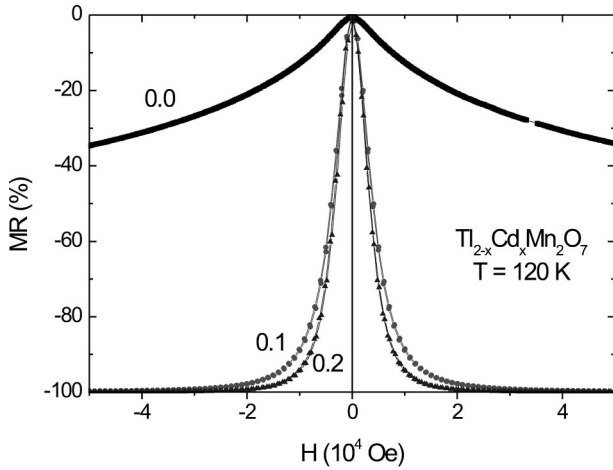


FIG. 5. Variation of the magnetoresistance ratio (MRI) with the applied magnetic field for $\text{Tl}_{2-x}\text{Cd}_x\text{Mn}_2\text{O}_7$, measured at 120 K (around the transition temperatures). Observe the large low-field magnetoresistance for the doped samples.

This drop in the resistivity with the application of a magnetic field is known as magnetoresistance. The MR ratio can be defined as $\text{MR}(H) (\%) = 100 \times [\rho(H) - \rho(0T)] / \rho(0T)$. As ρ decreases upon the application of a magnetic field, MR will be negative and the maximum available value is 100%. When this effect is huge, as it is the case, MR takes values above 99.9% and it is difficult to establish proper comparisons. For this reason, it is preferred to define it as $\text{MRI}(H) (\%) = 100 \times [\rho(H) - \rho(0T)] / \rho(H)$, allowing us to have a better idea of the magnitude of the change. In the upper part of the Fig. 4 we show the variation of the MRI at 9 T with the temperature for the three samples. One can appreciate the wide peak that appears about T_C (shadowed area). The temperature of the maximum $T(\text{MRI}_{\text{max}})$ slightly decreases in Cd samples (see Table III). This is coherent with the decrease in T_C , produced by a weaker FM interaction. The most spectacular result is that the maximum value of MRI is drastically increased with Cd doping. For the $\text{Tl}_{1.8}\text{Cd}_{0.2}\text{Mn}_2\text{O}_7$ sample, the maximum $\text{MRI}(9 \text{ T})$ is above $10^6\%$. To our knowledge, this is the highest magnetoresistance ratio ever reported in bulk oxides.¹⁰

Figure 5 represents MR versus the applied magnetic field, measured at 120 K. This temperature corresponds, approximately, to the maximum in MRI at 9 T, where the effect is more drastic. Notice that a small amount of Cd doping at Tl positions (5%) produces a spectacular change in magnetoresistance. Values above $10^4\%$ are achieved at fields of 2.5 and 1.5 T for $\text{Tl}_{1.9}\text{Cd}_{0.1}\text{Mn}_2\text{O}_7$ and $\text{Tl}_{1.8}\text{Cd}_{0.2}\text{Mn}_2\text{O}_7$, respectively. The low-field magnetoresistance is also very high: For $H = 1 \text{ T}$, MR increases from 10% for the pure compound, to $8 \times 10^2\%$ for $x = 0.1$ and to $2 \times 10^3\%$ for $x = 0.2$. This is also one of the highest MR ratios ever reported for this moderate magnetic field.

The Hall-effect data are shown in Fig. 6. The transverse resistivity slope is negative, implying that the conduction carriers are electrons. The increase in the slope when doping with Cd means that the number of carriers (n) is decreasing. The values of n are given in Table III, and plotted in the inset

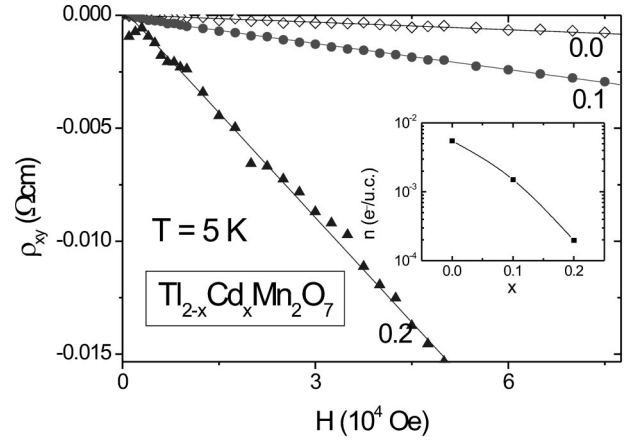


FIG. 6. Hall-effect measurements: variation of the transverse resistivity with the applied field, measured at 5 K, for the $\text{Tl}_{2-x}\text{Cd}_x\text{Mn}_2\text{O}_7$ compounds. Inset: variation of the number of carriers per unit cell with the Cd content (note the log scale).

of Fig. 6. The obtained figures are in agreement with the evaluation we made from the fitting of the high-temperature conductivity to an activated behavior. In addition, the effect of doping is very important, reducing the number of carriers in almost one order of magnitude from the lower doping level ($x = 0.1$) to the next one ($x = 0.2$). This reduction in the number of carriers is coherent with the increase of the resistivity upon Cd doping. We demonstrate below that it is also responsible for the magnitude of the changes observed in the magnetotransport properties.

Majumdar and Littlewood developed a model for the MR in a FM material with a low carrier density.²⁰ In such a material, the transport is governed above the transition temperature by scattering due to spin fluctuations. As the carriers are coupled to the localized moments, which is reflected in the formation of spin polarons, the transport occurs via polaron hopping. For temperatures well above T_C ($T > 1.2 T_C$), Majumdar and Littlewood²⁰ demonstrate that MR scales with the square of the magnetization, in the form

$$\Delta\rho/\rho_0 \approx C_{\text{Littlewood}} \left(\frac{m}{m_s} \right)^2,$$

where m_s is the saturation magnetization for that material. This scaling is independent of the temperature, as far as the model can be applied. The value of $C_{\text{Littlewood}}$ is proportional to the reciprocal of number of carriers $C_{\text{Littlewood}} \sim n^{-2/3}$.

In Fig. 7 we plotted the magnetoresistance $\Delta\rho/\rho_0$ versus the square of the magnetization, at several temperatures, for the three samples. The three plots are linear for small values of $(m/m_s)^2$. Also, the values of $C_{\text{Littlewood}}$ are independent of the temperature, assessing the goodness of the model. In addition, the increase in the slope $C_{\text{Littlewood}}$ with the doping level (see Table III) is coherent with the decrease in the number of carriers, as measured by the Hall effect and predicted by the model.

The specific heat around the magnetic transition for $\text{Tl}_2\text{Mn}_2\text{O}_7$ and $\text{Tl}_{1.8}\text{Cd}_{0.2}\text{Mn}_2\text{O}_7$ is plotted in Fig. 8, after subtraction of the phononic and electronic component. In

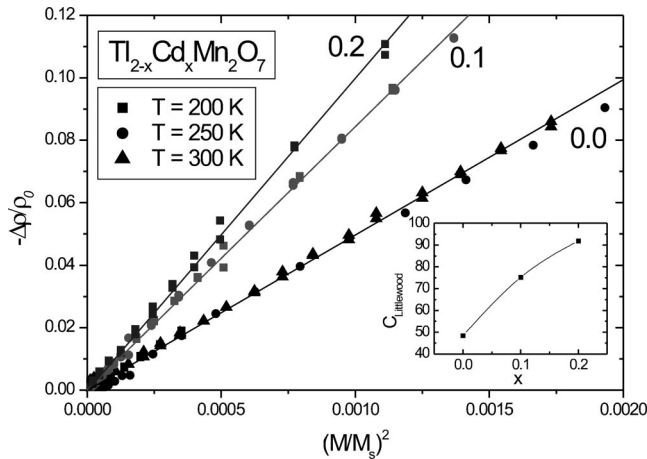


FIG. 7. Relation between the magnetoresistance and the square of the magnetization, for three different temperatures. The agreement with the Majumdar-Littlewood model is shown (lines). Inset: variation of the proportionality factor $C_{\text{Littlewood}}$ with the Cd content.

both samples, a well-defined peak corresponds to the magnetic ordering temperature T_C . In the case of the $x=0.2$ Cd-substituted material, the peak is displaced towards lower temperatures, as observed from susceptibility measurements. When a magnetic field is applied, there is a reduction of the height and a broadening of the peak, evidencing that the

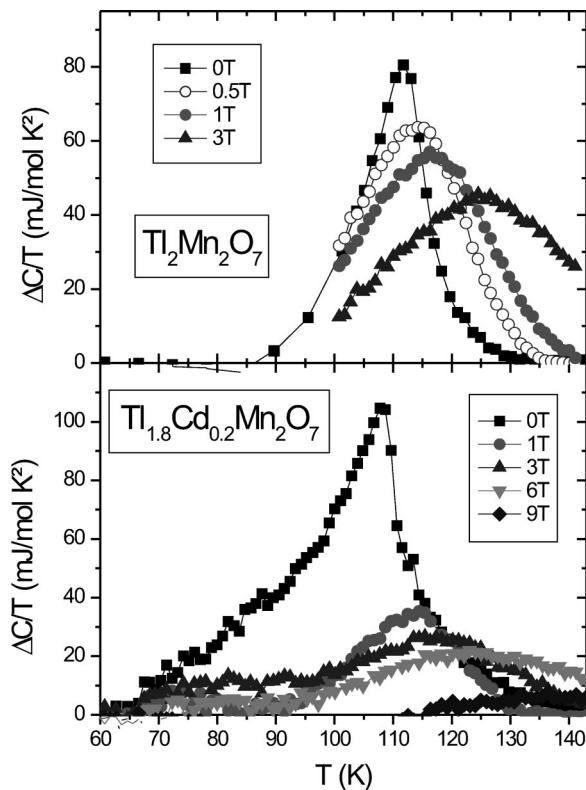


FIG. 8. Magnetic transition peak in the specific heat for $\text{Tl}_2\text{Mn}_2\text{O}_7$ (upper panel) and $\text{Tl}_{1.8}\text{Cd}_{0.2}\text{Mn}_2\text{O}_7$ (lower panel), for different applied magnetic fields (after subtracting the phononic and electronic components).

magnetic interactions extend to a higher temperature range, reaching larger T values. The integration of the peaks shows how much energy is involved in the transition, for each case. Under a zero magnetic field the peak area is larger for the $x=0.2$ Cd-doped sample (see Table IV), suggesting that more energy is required to align the Mn spins in parallel. As the saturation magnetization is almost the same for both samples, this result suggests that we have a weaker magnetic interaction in the Cd-doped sample, and hence, we need to supply more energy for reaching the magnetically ordered state.

Several mechanisms have been proposed as responsible for the magnetic interactions in $\text{Tl}_2\text{Mn}_2\text{O}_7$ derived materials. There is a general consensus excluding a DE mechanism, and accepting SE between neighboring Mn cations as the most possible driving force for magnetic ordering. Sushko *et al.* proposed a model²¹ in which the interactions between nearest neighbors are AF in origin, and that the interactions to next-nearest neighbors are indeed FM and dominate due to the geometrical frustration of the lattice. Recently, Núñez-Regueiro and Lacroix proposed²² that the magnetism in $A_2\text{Mn}_2\text{O}_7$ pyrochlores ($A=\text{In}, \text{Tl}$) can be explained as the superposition of two interaction terms. The first one is a conventional SE across Mn-O-Mn paths, which alone would not explain T_C values above 15 K. These authors²² introduce an additional indirect exchange term due to the overlapping of the conduction band with the $\text{Mn}(e_g)$ levels, in such a way that the conduction electrons indeed participate in the strengthening of the magnetic interactions. We have experimentally shown that this is the case in the $\text{Tl}_{2-x}\text{Cd}_x\text{Mn}_2\text{O}_7$ series, where a reduction in the strength of the FM interactions is observed upon Cd doping, concomitant with a decrease in the number of carriers and a dramatic increment in the MR ratio.

IV. DISCUSSION

The introduction of Cd^{2+} cations in the Tl^{3+} sublattice seems to suggest, within a simple ionic picture, a concomitant increase of the oxidation state of manganese cations, implying the oxidation of some Mn^{4+} to Mn^{5+} , assuming that the oxygen stoichiometry is unchanged. However, $\text{Tl}_2\text{Mn}_2\text{O}_7$ pyrochlore is certainly not an example of a “simple ionic” compound. As demonstrated by electronic band-structure calculations¹⁸ in this compound there exists a majority conduction band, with heavy holes that do not contribute to the transport and a minority conduction band, with light electrons that are the responsible for the transport and the magnetic interactions (see Fig. 9). The existence of this minority conduction band means that electrons are not totally located at the oxygen ions, but instead a part of them is delocalized, as it happens in a metal. This can be seen as an “increase” in the oxidation state for the oxygen, implying that the transfer of two electrons from the metal elements into the oxygen has not been completed in this compound, better named as “half-metallic.”

In a first approximation we can assume that the introduction of Cd^{2+} at Tl^{3+} sites will not significantly change the band structure, instead leading to a lower filling in the conduction band. The charge neutrality is preserved, since each

TABLE IV. Specific heat parameters for $\text{Tl}_2\text{Mn}_2\text{O}_7$ and $\text{Tl}_{1.8}\text{Cd}_{0.2}\text{Mn}_2\text{O}_7$, measured at different magnetic fields (see Fig. 8).

Sample	$\text{Tl}_2\text{Mn}_2\text{O}_7$			$\text{Tl}_{1.8}\text{Cd}_{0.2}\text{Mn}_2\text{O}_7$			
	Magnetic field (T)	Peak area (J/mol K)	T (K)	Peak width (K)	Peak area (J/mol K)	T (K)	Peak width (K)
0		1.239	111.72	13.24	2.616	107.74	17.33
0.5		1.311	114.18	21.81			
1		1.375	116.25	25.89	0.836	114.4	20.2
3		1.352	124.54	33.10	1.114	115.4	51.7
6					0.994	123.1	44.1
9					0.202	136.5	30.6

Tl^{3+} will contribute with three electrons to the filling of the bands and the Cd^{2+} will do the same with two electrons. Consequently, the number of positive charges located at the cations is equivalent to the number of electrons in the bands of the solid.

Mn contributes with four electrons; therefore, for the pure $\text{Tl}_2\text{Mn}_2\text{O}_7$ compound, the total number of transferred electrons is $3 \times 2 + 4 \times 2 = 14$. A part is located in the inner bands, and only the last electron is to be considered for our purposes (responsible for the transport properties of this material). A fraction of this very last electron is in the minority conduction band, and this fraction is the one measured by Hall effect ($n = 6.87 \times 10^{-4}$ e/f.u., at 5 K, see below). The rest of this last electron is, therefore, in the majority conduction band.

When substituting x atoms of Tl^{3+} by Cd^{2+} , the total number of electrons provided per formula is $14 - x$. Thirteen of them will occupy the inner bands, and the rest $(1 - x)$ will be the topmost ones, responsible for the properties of interest. For the pure pyrochlore ($x = 0$) a 6.87×10^{-4} fraction of this last electron is in the minority band, and 0.99313 of it is in the majority. When introducing x Cd atoms we can assume, again in a first approximation, that this ratio is similar to that observed in the undoped compound. That makes that in the minority band, contributing to the transport, there are

$(1 - x) \times 6.87 \times 10^{-4}$ electrons per formula unit. For Cd 0.1, this number is $0.9 \times 6.87 \times 10^{-4} = 6.18 \times 10^{-4}$ e/f.u. Experimentally, from Hall data, we found $n_{0.1} = 1.9 \times 10^{-4}$ e/f.u. (see below). For Cd 0.2 the number is $0.8 \times 6.87 \times 10^{-4} = 5.5 \times 10^{-4}$ e/f.u. From Hall data we found $n_{0.2} = 0.25 \times 10^{-4}$ e/f.u. (see below). We always observe a number of charge carriers lower than expected.

The differences observed between the experimental (Hall) and expected number of carriers can be understood by examining the introduced simplifications, (i) the ratio of electrons in the minority and majority conduction bands will not be constant when introducing Cd, since the bands are parabolic, and the number of electrons in the minority bands will be lower as the total number of electrons is reduced and (ii) the band structure indeed changes, since Cd tends to form more ionic, undirected bonds in the solid, thus narrowing the bands in the proximity of Cd sites, introducing scattering centers, and reducing the effective number of carriers we measure.

Moreover, the Cd inclusion not only changes the number of carriers, but—as we explained before—it produces a narrowing of the bands in the neighborhood of the Cd cations. That affects the spin-separated transport. That is, reaching a Cd site, the number of minority electrons will be reduced (as the band increases in energy), and some electrons will go to the majority band. But this mechanism involves a spin-flip process. Therefore, there are local spin scattering centres, introduced by Cd, that will reduce the electron mobility.

Let us consider the relative influence of both magnitudes, number of carriers, and mobility, in the resistivity and magnetoresistance of these materials. In Fig. 10 we give the temperature evolution of the number of carriers for the different samples. Note the significant decrease of this magnitude, especially around T_C . This can explain, in part, the increase in the resistivity near T_C . Regarding the influence of the mobility of the carriers in the changes in the resistivity, let us first consider the variation of the resistivity with the temperature. In Table V we give the number of carriers and the resistivity for different temperatures. As the conductivity σ is given by $\sigma = ne\mu_e$, we can calculate the electron mobility μ_e from the experimental values (see also Table V). When heating from low temperatures, the mobility decreases by 5 orders of magnitude at the peak in the resistivity (120 K), and increases slightly due to the enhancement of the ther-

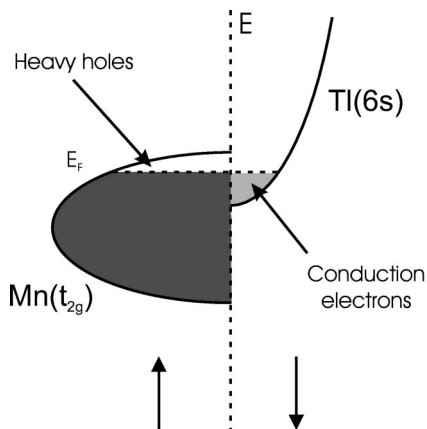


FIG. 9. Schematic density of states of the pyrochlore $\text{Tl}_2\text{Mn}_2\text{O}_7$, as proposed by Singh (Ref. 18). Up (down) arrow indicate majority (minority) spins.

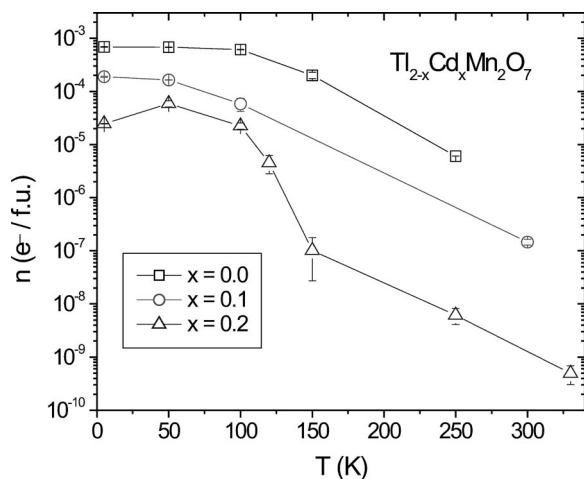


FIG. 10. Evolution of the number of carriers per formula unit, measured by Hall effect, with the temperature, for $\text{Tl}_{2-x}\text{Cd}_x\text{Mn}_2\text{O}_7$.

mally activated movement of the polarons. This produces the decay in the resistivity at high temperatures.

Let us finally discuss on the influence of the mobility on the magnetoresistance. As mentioned in the results section, the conductivity of the electrons is tightly bound to the parallel alignment of the magnetic moments, in such a way that the application of a magnetic field near the transition temperature considerably aligns the magnetic moments, inducing a clear increase in the mobility. It is very difficult to estimate this effect directly: as the resistivity is proportional to the reciprocal of both n and ρ , the decrease in the resistivity upon the application of a magnetic field (magnetoresistive effect) can be due to an increase either in the number of carriers, or in the mobility, or in both magnitudes, when an external magnetic field is applied. The only way to separate the intrinsic variation of the mobility with the field is by measuring the variation of both the resistivity and the number of carriers. The variation of the resistivity is given by the MR ratio, in Figs. 4 and 5. An increase in the number of carriers with the magnetic field will lead to a decrease in the slope value in the transverse resistivity. For high temperatures, near T_C , it is very difficult to properly estimate the number of carriers, mainly due to the great increase in the MR, and the appearance of considerable anomalous contri-

TABLE V. Variation of the number of carriers (n), the resistivity (ρ), and the electron mobility (μ_e) of the $\text{Tl}_{1.8}\text{Cd}_{0.2}\text{Mn}_2\text{O}_7$ compound with the temperature.

T (K)	$\text{Tl}_{1.8}\text{Cd}_{0.2}\text{Mn}_2\text{O}_7$		
	n ($e^- \text{m}^{-3}$)	ρ (Ωm)	μ_e (m^2/Vs)
5	2.03×10^{23}	2.90×10^{-3}	10.61×10^{-3}
120	3.79×10^{22}	1.54×10^3	1.1×10^{-7}
250	6.84×10^{19}	3.92×10^2	2.3×10^{-4}

butions. At low temperatures there is no appreciable effect (Fig. 6), therefore, we can conclude that n does not vary with the field, and that the magnetoresistive effect is due to an increase in the mobility upon the application of a magnetic field.

V. CONCLUSIONS

We have performed an in-depth study of the magnetic, transport and magnetotransport properties of the $\text{Tl}_{2-x}\text{Cd}_x\text{Mn}_2\text{O}_7$ pyrochlores family, with $0 \leq x \leq 0.2$. A huge increase in MR is progressively observed upon Cd doping. The magnetic properties and specific heat measurements present evidence for a weakening of the strength of the FM interactions. Transport measurements reveal a drastic decrease in the number of carriers in the Cd-substituted materials. The fit of the magnetotransport data to the Majumdar-Littlewood model allows us to conclude that the MR response in these materials is correlated to the magnetic interactions, and that the large increase of MR and the weakening of the magnetic interactions are both related to the decrease in the number of carriers. A NPD study, showing that Cd replaces at random Tl atoms, suggests a larger ionic contribution in the average (Tl, Cd)-O bonds, leading to a reduced electronic transfer to the conduction band, thus dramatically decreasing the number of carriers available for electronic transport.

ACKNOWLEDGMENTS

We thank the financial support of the spanish Ministerio de Ciencia y Tecnología to the Projects No. MAT2001-0539 and MAT99-1045, and we are grateful to ILL for making all facilities available.

¹R. Von Helmlont, J. Wecker, B. Holzapfel, L. Schultz, and K. Samwer, Phys. Rev. Lett. **71**, 2331 (1993).

²Y. Shimikawa, Y. Kubo, and T. Manako, Nature (London) **379**, 53 (1996).

³S.-W. Cheong, H. Y. Hwang, B. Batlogg, and L. W. Rupp, Solid State Commun. **98**, 163 (1996).

⁴M. A. Subramanian, B. H. Toby, A. P. Ramirez, W. J. Marshall, A. W. Sleight, and G. H. Kwei, Science **273**, 81 (1996).

⁵A. P. Ramirez and M. A. Subramanian, Science **277**, 546 (1997).

⁶H. Y. Hwang and S.-W. Cheong, Nature (London) **389**, 942 (1997).

⁷M. A. Subramanian, A. P. Ramirez, and G. H. Kwei, Solid State Ionics **108**, 185 (1998).

⁸M. A. Subramanian, G. Aravamudan, and G. V. Subba Rao, Prog. Solid State Chem. **15**, 55 (1983).

⁹J. A. Alonso, J. L. Martínez, M. J. Martínez-Lope, M. T. Casais, and M. T. Fernández-Díaz, Phys. Rev. Lett. **82**, 189 (1999).

¹⁰J. A. Alonso, P. Velasco, M. J. Martínez-Lope, M. T. Casais, J. L. Martínez, M. T. Fernández-Díaz, and J. M. de Paoli, Appl. Phys. Lett. **76**, 3274 (2000).

¹¹B. Martínez, R. Senis, J. Foncuberta, X. Obradors, W. Cheihk-

- Rouhou, P. Strobel, C. Bougerol-Chaillout, and M. Pernet, *Phys. Rev. Lett.* **83**, 2022 (1999).
- ¹²J. A. Alonso, M. J. Martínez-Lope, M. T. Casais, P. Velasco, J. L. Martínez, M. T. Fernández-Díaz, and J. M. de Paoli, *Phys. Rev. B* **60**, R15 024 (1999).
- ¹³P. Velasco, J. A. Alonso, M. J. Martínez-Lope, M. T. Casais, J. L. Martínez, M. T. Fernández-Díaz, and J. M. de Paoli, *Phys. Rev. B* **64**, 184436 (2001).
- ¹⁴P. Velasco, J. A. Alonso, M. J. Martínez-Lope, M. T. Casais, J. L. Martínez, M. T. Fernández-Díaz, and J. M. de Paoli, *J. Phys.: Condens. Matter* **13**, 10 991 (2001).
- ¹⁵R. D. Shannon, *Acta Crystallogr., Sect. A: Found. Crystallogr.* **32**, 751 (1976).
- ¹⁶J. Rodríguez-Carvajal, *Physica B* **192**, 55 (1993).
- ¹⁷J. A. Alonso, M. J. Martínez-Lope, M. T. Casais, J. L. Martínez, and M. T. Fernández-Díaz, *Chem. Mater.* **12**, 1127 (2000).
- ¹⁸D. J. Singh, *Phys. Rev. B* **55**, 313 (1997).
- ¹⁹S. H. Chun, M. B. Salamon, Y. Tomioka, and Y. Tokura, *Phys. Rev. B* **61**, R9225 (2000).
- ²⁰P. Majumdar and P. B. Littlewood, *Nature (London)* **395**, 479 (1998).
- ²¹Yu. V. Sushko, Y. Kubo, Y. Shimakawa, and T. Manako, *Physica B* **259–261**, 831 (1999).
- ²²M. D. Núñez-Regueiro and C. Lacroix, *Phys. Rev. B* **63**, 014417 (2001).